Quarterly Journal of the Royal Meteorological Society

Q. J. R. Meteorol. Soc. 140: 480–490, January 2014 B

RMetS

Royal Meteorological Society

The convective adjustment time-scale as indicator of predictability of convective precipitation

Christian Keil,[a]* Florian Heinlein[a,b] and George C. Craig[a]

[a]*Meteorologisches Institut, Ludwig-Maximilians-Universität, Munich, Germany*
[b]*Hans-Ertel-Centre for Weather Research, Data Assimilation Branch, Ludwig-Maximilians-Universität, Munich, Germany*

*Correspondence to: C. Keil, Meteorologisches Institut, LMU München, Theresienstr. 37, 80333 Munich Germany.
E-mail: christian.keil@lmu.de*

Predictability of convective precipitation depends on the interaction between synoptic forcing and local-scale flow characteristics. In order to assess different predictability levels it is desirable to objectively determine the dominant process in a given meteorological situation. Such a measure is given by the convective adjustment time-scale τ, a physically based quantity that distinguishes between strong and weak synoptically forced precipitation regimes. By employing the convective adjustment time-scale diagnostic, forecasts of the convection-permitting COSMO-DE ensemble prediction system available for a total of 88 days in summer 2009 are examined. Based on the normalized ensemble spread of hourly precipitation rates, it is shown that the practical predictability of total precipitation is higher during strong large-scale forcing than during weak forcing. Likewise, the forecast skill, determined using two deterministic scores, is higher during strong than during weak forcing conditions. Different predictability levels of convective precipitation can be revealed by examining distinct sub-ensembles depending on their source of uncertainty. The impact of variations in the boundary conditions of the driving global models used in the ensemble system is quite insensitive to the prevailing flow regime, while the impact of physics perturbations representing the model error is clearly weather regime dependent, exhibiting a strong contribution only during weakly forced conditions. Then convective precipitation turns out to be especially sensitive to variations in the physics parametrization even at forecast lead times of 12 to 18 hours during the main convective period in the afternoon. Two case-studies exemplifying the strong and weak forcing regimes are shown, to illustrate how forecast skill varies and the different ensemble members cluster as the precipitation event evolves.

1. Introduction

In meteorology the term 'predictability' describes the characteristic of atmospheric weather prediction models being sensitive to errors in initial conditions (Thompson, 1957), boundary conditions and model error. Early work by Lorenz and others during the 1960s and 1970s focused on weather and the state of the midlatitude troposphere and provides a framework regarding forecasting and predictability. Lorenz defined predictability as 'a limit to the accuracy

with which forecasting is possible' (Lorenz, 1969). He later refined his view, providing two aspects of predictability: 'intrinsic predictability – the extent to which the prediction is possible if an optimum *procedure* is used' and 'practical predictability – the ability to predict based on the *procedures* currently available' (Lorenz, 2006; Zhang *et al.*, 2006).

In the last decade, high-resolution atmospheric models with kilometre-scale horizontal mesh sizes where deep convection is represented explicitly rather than by a convection parametrization have been put in operation at many meteorological services (e.g. Davies *et al.*, 2005; Baldauf *et al.*, 2011; Seity *et al.*, 2011). These non-hydrostatic, convection-permitting weather forecast models improve the realism and forecast quality of precipitation (Kain *et al.*, 2008; Lean *et al.*, 2008; Rotach *et al.*, 2009; Weusthoff *et al.*, 2010). Now, the application of short-range convection-permitting models calls for an examination of both aspects of predictability of the simulated small-scale atmospheric phenomena, since the time-scale of atmospheric instabilities is related to their spatial scales, and small-scale instabilities grow much faster than those with larger scales (Kalnay, 2003). The spatio-temporal highly variable and intermittent precipitation field exhibits a characteristic fingerprint of such small-scale instabilities.

Quantifying the predictability of precipitation forecasts associated with new forecasting *procedures* (i.e. convection-permitting models) is therefore an important issue (Errico *et al.*, 2002). Intrinsic predictability can be studied using a perfect model assumption in conjunction with tiny initial condition uncertainties (i.e. uncertainties an order of magnitude smaller than the analysis error) and examining the error growth (e.g. Zhang *et al.*, 2003, 2006; Bei and Zhang, 2007). Practical predictability can be examined with ensemble prediction systems that sample the different sources of uncertainty. In general, ensemble forecasts aim to span the space of possible scenarios by perturbing the different sources with realistic values and aim to provide a measure of confidence in the forecast.

The usefulness of limited-area ensemble prediction systems at mesh sizes of the order of 10 km in terms of quantitative precipitation forecasting (e.g. Marsigli *et al.*, 2004; Bowler *et al.*, 2008; Montani *et al.*, 2011) has fostered the development of convection-permitting ensembles at kilometre-scale resolution. Clark *et al.* (2009) compared the precipitation forecast skill between a convection-parametrizing ensemble and a convection-permitting ensemble and found superior skill for the high-resolution ensemble comprising fewer members. They conclude that it is highly desirable to increase the ensemble resolution even at the expense of reducing the ensemble size for given computational resources. Similarly, Hohenegger *et al.* (2008) compared the performance of a regional, convection-parametrizing ensemble system with a convection-permitting ensemble for the August 2005 Alpine flood event. They showed that the benefit of convection-permitting ensembles depends on the synoptic situation.

Predictability of total precipitation strongly depends on both the synoptic-scale circulation patterns and local-scale flow characteristics. Under strong synoptic forcing (e.g. along fronts or on the leading edge of upper-level troughs) the precipitation is often associated with large-scale ascent that cools the troposphere and creates conditional instability. These situations are often realistically captured by high-resolution models resulting in a comparatively high forecast quality. When precipitation is controlled by synoptic scales, precipitation is more predictable (e.g. Roebber *et al.*, 2008) and, hence, its forecast uncertainty is relatively low. Conversely, when precipitation is governed by local-scale flow characteristics and the interaction with the synoptic flow is weak (e.g. during air-mass convection situations beneath a high-pressure ridge in a weak gradient field of equivalent potential temperature) the forecast quality of precipitation is lower. That is, precipitation during these weather regimes is less predictable and forecast uncertainty is high (Zhang *et al.*, 2006; Trentmann *et al.*, 2009; Barthlott *et al.*, 2011). Under these weakly forced flow conditions, local-scale processes such as solar insolation, local orography or different vegetation cover and their complex interactions can lead to surface flux variability and thermally driven wind systems. Emerging convergence lines in the boundary layer can be sufficient to overcome an existing energy barrier (convective inhibition, CIN) to release the available convective instability (convective available potential energy, CAPE) and trigger precipitation processes in the absence of synoptic-scale forcing.

Stensrud *et al.* (2000) studied the development of two mesoscale convective systems with regional, convection-parametrizing ensembles. They found that the initial condition ensemble is more skilful than the model physics ensemble when the synoptic forcing is strong, while the model physics ensemble shows more skill when the synoptic forcing for upward motion is weak. Schwartz *et al.* (2010) evaluated precipitation forecasts of a convection-permitting ensemble employing the WRF (Weather Research and Forecasting) model during the National Oceanic and Atmospheric Administration (NOAA) Spring Experiment 2007. Validating 12-hourly accumulated rainfall totals for a 35-day period across the continental United States, they found that initial conditions play an important role in modulating the precipitation and that precipitation spread can be achieved by varying the physical parametrizations within an ensemble system. Vié *et al.* (2011) studied the forecast uncertainty of Mediterranean heavy precipitation events perturbing convective-scale initial conditions and lateral boundary conditions in the convection-permitting AROME (Application of Research to Operations at Mesoscale) model. They concluded that the synoptic circulation plays a dominant factor controlling the relative impact of both perturbations. In the case of strong synoptic forcing the impact of the uncertainty in the lateral boundary conditions (LBC) is predominant, while in the case of weaker large-scale circulation the impact of the convective-scale perturbations introduced at initial time is enhanced.

A multi-parameter and multi-boundary approach to focus on uncertainties in model physics and LBCs has been developed at Deutscher Wetterdienst (DWD) based on the convective-scale COSMO-DE (Consortium for Small Scale Modelling) model (Gebhardt *et al.*, 2011). Using these COSMO-DE-EPS (Ensemble Prediction System) forecasts covering a 15-day period in summer 2007 they concluded that the impact of the physics perturbations dominates during the first six hours of the forecast, but can also be relevant at longer lead times in some cases.

In many studies the classification in a strongly or weakly synoptic forced flow regime is based on a subjective forecaster-based analysis of the meteorological situation. For instance, Vié *et al.* (2011) used the mean 500 hPa wind speed at a 12 hours forecast range above or below the

monthly median to delineate days with strong or weak synoptic forcing conditions. This may be feasible for a limited amount of case-studies, but becomes infeasible for longer periods. Thus it is desirable to objectively distinguish the different modes of interaction between synoptic forcing and convection and to determine the dominant process in a given meteorological situation. The convective adjustment time-scale constitutes such a measure to discern different flow regimes (see detailed description in next section). Recently, Keil and Craig (2011) applied this physically based measure to determine prevailing meteorological conditions during summertime convection. Using COSMO-DE-EPS forecasts on nine consecutive days in summer 2007 they examined the regime-dependent forecast uncertainty of precipitation and suggested the convective adjustment time-scale as a suitable predictor of the flow regime and, hence, forecast uncertainty of convective precipitation.

In this study the hypothesis that the convective adjustment time-scale indicates forecast uncertainty of precipitation is verified using ensemble forecasts of an entire summer period in central Europe. The following questions are addressed: Do the two sources of uncertainty represented in the COSMO-DE-EPS system influence practical predictability differently depending on the type of forcing? Is the forecast uncertainty more sensitive to LBCs during precipitation situations associated with strong synoptic forcing by midlatitude weather systems? And conversely: Are the physics perturbations more important during air-mass convection situations, when convective precipitation is triggered by local, small-scale processes under weak large-scale forcing?

The structure of the article is as follows. Section 2 describes the convective adjustment time-scale τ. In section 3 the convection-permitting ensemble system, the observational data, the applied methodology and the examined period are described. Section 4 comprises the results containing a climatological classification of the summer 2009, an analysis of weather regime dependent practical predictability and forecast quality exploiting the full ensemble, and an assessment of the impact of different sources of uncertainty by comparing different sub-ensembles. In section 5 distinct case-studies illustrate the regime-dependent forecasting characteristics during both weather conditions. A summary and an outlook are given in section 6.

2. The convective adjustment time-scale τ

To some degree convective precipitation is under the control of the large-scale environment. Primarily two scenarios can be distinguished. First, in the presence of strong synoptic forcing, the amount of convection is determined by the rate at which conditional instability (CAPE) is produced by large-scale ascent cooling the troposphere. As long as CAPE is available, convection will occur and remove CAPE with a time-scale of about one hour. In this case, the amount of convection is closely linked with the synoptic forcing. Second, in the absence of synoptic forcing, local processes in the boundary layer are essential to overcome the energy barrier of convective inhibition (CIN) in order to trigger convection. Even in the presence of CAPE, convection will not occur if triggering mechanisms initiating convection are missing during weak large-scale forcing. In this case, the amount of convection is controlled by the interaction of triggering processes and CIN, and no close relationship between the larger scales and convection is expected.

The convective adjustment time-scale τ represents a measure to distinguish the different flow regimes. It is an estimate of the time-scale for the removal of conditional instability (measured by CAPE) by convective heating:

$$\tau = \frac{CAPE}{dCAPE/dt}$$

Following Done *et al.* (2006), the rate of change of CAPE can be expressed by the vertically integrated latent heat release that, in turn, can directly be determined from the precipitation rate $P\,(\mathrm{kg\,s^{-1}\,m^{-2}})$. The convective adjustment time scale τ can be estimated as

$$\tau = 0.5 \left(\frac{\rho_0 c_p T_0}{L_v g} \right) \frac{CAPE}{P},$$

with the quantities in brackets being constants (ρ_0 and T_0 are reference values of density and temperature, c_p the specific heat of air at constant pressure, L_v the latent heat of vaporization, and g the acceleration due to gravity (e.g. Zimmer *et al.*, 2011)). If τ is only a few hours and therefore short compared to the time-scale over which the large-scale flow evolves (say 12 hours), the convection will remove CAPE as fast as it is created, and the rate of creation of CAPE controls the amount of convection. On the other hand, if τ is similar to, or longer than 12 hours, convection is acting too slowly to remove the CAPE, and there must be local factors controlling its rate. It is important to note, however, that the resultant convective adjustment time-scale value should not be taken at face value; it rather gives an estimate to classify the prevailing meteorological regime with strong and weak forcing situations being extremes of a continuous distribution. Since the convective adjustment time-scale is determined by the ratio of CAPE and precipitation rate, it is sensitive to the specific calculation of both ingredients. A reasonable threshold to distinguish between the prevailing regimes would be between 3 and 12 hours, but the precise value is not crucial since the vast majority of values are either larger or smaller than this range (Zimmer *et al.*, 2011).

Using COSMO-DE forecast data, τ is computed using the mean layer CAPE (based on the mean temperature and humidity of the lowest 50 hPa following Leuenberger *et al.* (2010)) and hourly total precipitation rates. Since the time-scale represents an environment in which convection occurs, both fields are smoothed with a Gaussian kernel (with a half-width size of 56 km) prior to its calculation. An hourly, area-averaged convective adjustment time-scale is calculated conditional to COSMO-DE grid points receiving more than 1 mm rainfall per hour to exclude dry areas where τ cannot be computed.

The measure of the convective adjustment time-scale τ has already been successfully applied to examine ensemble bias and spread of precipitation (Done *et al.*, 2006, 2011; Keil and Craig, 2011), to assess the length of impact of radar data assimilation in COSMO-DE (Craig *et al.*, 2012), to distinguish the skill of probabilistic forecasts (Kober *et al.*, 2013), to study severe precipitation events in the Mediterranean using re-analysis data (Molini *et al.*, 2011) and to classify observed summertime precipitation (Zimmer *et al.*, 2011).
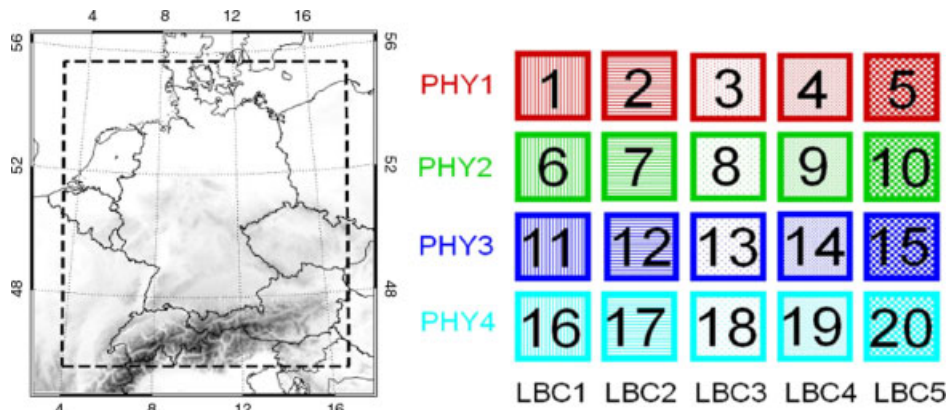
Figure 1. Domain of COSMO-DE-EPS with coastlines, political boundaries and topographic heights of the model orography (left). The dashed square indicates the verification domain of quantitative precipitation forecasts. The design of COSMO-DE-EPS is characterized by the same global model in the rows and the same physics perturbation in the columns (right). For instance, the sub-ensemble PHY1 consists of members 1 to 5 driven with the same ECMWF LBC but variable physics perturbation. PHY2 is driven by the global model of DWD, PHY3 by NCEP and PHY4 by UKMO, while the different columns consist of members having the same physics perturbation but different LBC: LBC1 with perturbed entrainment rate for shallow convection, LBC2 with critical value for oversaturation, LBC3 and LBC4 by different scaling factor of the laminar boundary layer for heat and LBC5 by asymptotic mixing length of turbulence. This figure is available in colour online at wileyonlinelibrary.com/journal/qj

3. Data and methods

3.1. The limited-area ensemble prediction system

In the present study, ensemble forecasts of the COSMO-DE-EPS performed at DWD are examined. In COSMO-DE-EPS the non-hydrostatic convection-permitting COSMO-DE model (Baldauf *et al.*, 2011; $\Delta x = 2.8$ km) is put in ensemble mode by following a multi-parameter and multi-boundary approach to include uncertainties in model physics and LBCs (Gebhardt *et al.*, 2011). Uncertainties in the LBCs stem from the COSMO-SREPS (Marsigli *et al.*, 2008; $\Delta x = 10$ km) which itself is driven by the four global models run at the European Centre for Medium-range Weather Forecasts (ECMWF), the DWD, the National Centers for Environmental Prediction (NCEP) and the UK Met Office, respectively. The five physics perturbations are accomplished in a non-stochastic and uniform approach by varying one parameter for each perturbation (see details in Fig. 1 and Tab. I of Peralta *et al.* (2012), respectively). These parameters are chosen to maximize the variability of convective precipitation. The matrix structure of the 20-member COSMO-DE-EPS is depicted in Figure 1, where the rows represent the four global models and the columns the five physics perturbations. COSMO-DE-EPS forecasts are started daily at 0000 UTC based on the operational COSMO-DE analysis (including data assimilation) with a forecast range of 24 hours. Here hourly precipitation rates of all forecast lead times are examined. Note that COSMO-DE-EPS was experimental at the time of the current study and the set-up used here does not completely represent its current operational (since 22 May 2012) status.

For validation purposes synthetic radar reflectivity at the 850 hPa pressure surface is used as a proxy for precipitation intensity that is calculated with a forward operator using information from the hydrometeor distribution of rain, snow and graupel at every grid point of the model (Seifert and Beheng, 2006). It forms the basis to assess forecast quality employing a mosaic of observed radar reflectivity data.

3.2. Radar observations

Forecast quality is validated using hourly radar reflectivity data of the *European radar composite*. This continental radar mosaic covers an area of 1800×1800 km^2 over Europe including the entire COSMO-DE domain. It delivers instantaneous radar intensities given in six reflectivity classes (7, 19, 28, 37, 46, 55 dBZ) at a horizontal resolution of 2 km and is mapped on the model grid for comparison. The threshold to calculate the quality is 19 dBZ which corresponds to a rain rate of 1 mm h^{-1}, and is identical to the threshold used to compute the area-averaged convective adjustment time-scale.

3.3. The methodology

The evaluation region covers the COSMO-DE domain excluding a frame of 32 grid points to allow for a clean Gaussian kernel averaging and to discard possible edge effects (Figure 1). This results in an area of 1090×1200 km^2 encompassing central Europe, extending from Paris to Vienna and Milan to Copenhagen. In order to address the open questions, certain sub-ensembles sharing the same LBCs or the same physics perturbation as well as individual members are evaluated besides the full ensemble. For instance, the members 1−5 driven by ECMWF form the PHY1 sub-ensemble, since the variability within this group stems from the different physics perturbations using identical LBCs (corresponding to e.g. the physics ensemble in Stensrud *et al.* (2000)), or members 5, 10, 15, 20 run with the same perturbed turbulent mixing length form the sub-ensemble LBC5 obtaining the variability from different LBCs (Figure 1).

To assess the precipitation forecast quality the examination is conducted using two widely used categorical deterministic scores. The frequency bias index (FBI) measures relative frequencies of precipitation rates exceeding a threshold and gives an indication of an over- (FBI > 1) or underestimation (FBI < 1) of precipitation (WMO, 2012). The equitable threat score (ETS) measures the fraction of events exceeding a threshold at individual grid locations

in either model or observation (Wilks, 2006). A similar validation methodology has been performed by Kong *et al.* (2009). Since the aim of the current study is the examination of regime-dependent practical predictability employing the convective adjustment time-scale, relative differences of forecast precipitation rates of the individual members or sub-ensembles are relevant. More sophisticated spatial verification measures avoiding the 'double-penalty' problem, like upscaling, the fractional skill score (Roberts and Lean, 2008; Weusthoff *et al.*, 2010) or probabilistic verification measures are not applied here.

As a measure of predictability, a normalized ensemble spread S_n of the precipitation rate P is calculated for the full ensemble and the different sub-ensembles:

$$S_{n,P} = \frac{1}{\bar{P}}\sqrt{\frac{1}{N-1}\sum_{i=1}^{N}(P_i - \bar{P})^2}.$$

The ensemble spread S is normalized with the mean value of the according (sub-)ensemble $\bar{P}$ to account for the large variability of the simulated precipitation rates. It is in some ways similar to Hohenegger *et al.* (2006) who compared the predictability as measured by ensemble spread for three cases of heavy precipitation.

3.4. *Period and model data availability*

The dataset of the present study consists of daily 24-hour ensemble forecasts between 20 May and 31 August 2009 (104 days in total) characterized by frequent precipitation episodes in central Europe. On 84% of these days forecasts of 10 or more ensemble members are available, on 31 days the entire 20-member ensemble. This heterogeneous data availability stems from the, at this time, still experimental character of the forecasts and their dependence on the timely provision of LBCs from four different global models. The forecast ensemble mean area-averaged precipitation exceeds 0.1 mm day^{-1} on 93% of the days. Inspection of the hourly precipitation rates throughout the period proves the predominant convective nature of summertime precipitation in central Europe. In 94% of the time when precipitation is forecast the ensemble mean area-averaged CAPE exceeds 10 J kg^{-1}.

4. **Results**

4.1. *Temporal partition of strongly and weakly forced meteorological conditions*

Statistics of area-averaged hourly ensemble mean COSMO-DE-EPS convective adjustment time-scales are used to put the summer 2009 in a 'climatological' context employing the analysis of Zimmer *et al.* (2011). Based upon observational data of seven warm seasons in Germany, they found that the strong and weak synoptic forcing situations can be regarded as extremes of a continuous distribution, with half to two thirds of summertime convective events occurring during strongly forced conditions ($\tau < 6$ (12) hours in 52% (59%) of the time). This analysis is based upon up to four radiosonde ascents per day at seven German locations used to calculate CAPE, as well as rain-gauges and radar data to estimate precipitation rates within a radius of 50 km around the sounding locations.

Based upon COSMO-DE-EPS forecasts the hourly ensemble mean convective adjustment time-scale, averaged across the model domain, classifies 67% (80%) of the events as strong synoptic forcing when applying a threshold of $\tau < 3$ (6) hours in summer 2009, respectively. This is consistent with the perception of weather conditions in summer 2009 being mainly governed by upper-level troughs and corresponding forced frontal precipitation in central Europe (e.g. DWD, 2010). Note, however, that the higher percentage of strong synoptic forcing conditions found here is partly attributable to a model bias in COSMO-DE CAPE and precipitation forecasts (Baldauf *et al.*, 2011). Another possible contribution to the difference emerges from the averaging procedure: regions of large and small τ are intermixed within the spatial averaging area covering 1090×1200 km^2 in the model, whereas a discrete point- or disk-like nature of the observations is used in Zimmer *et al.* (2011). When, for instance, strong synoptic forcing is present (corresponding to small τ over large regions) north of the German low mountain range, and in southwest Germany deep convection occurs under weak synoptic forcing (resulting in locally large values of τ), the domain-averaged τ is smoothed out. Finally, the observational study was restricted to the four standard radiosonde launch times, whereas all parts of the diurnal cycle are considered here.

Depending on the specific calculation method (as outlined above using COSMO model data or observations) the precise threshold value of the convective adjustment time-scale to classify into distinct weather regimes may vary, but ranges between 3 and 12 hours, respectively. While Zimmer *et al.* (2011) found a ratio of 2:1 between the occurrences of strongly and weakly forced meteorological conditions considering a threshold of 12 hours, the present analysis suggests a threshold of 3 hours to split the prevailing weather regimes accordingly using COSMO data. A threshold at the lower bounds of the $3-12$ hours range suggested by Zimmer *et al.* (2011) is compensating for the model bias.

4.2. *Weather regime dependent predictability and forecast quality*

As a measure of predictability the normalized ensemble spread of precipitation of the full 20-member ensemble is considered. A large (small) spread indicates poor (good) predictability. Hohenegger *et al.* (2006) call weather situations with a normalized precipitation spread close to 1 virtually unpredictable and situations with values close to 0.05 highly predictable. In Figure 2 the normalized spread of the area-averaged hourly precipitation rate covering all lead times is plotted against the corresponding area-averaged hourly convective adjustment time-scale τ for the entire period. At first glance, the scatterplot shows a general connection between τ and the precipitation spread, with small τ corresponding to a lower normalized spread and large τ to higher spread values. In order to highlight the different behaviour a threshold of 3 hours for the area-averaged convective adjustment time-scale is employed to separate different weather regimes. For $\tau < 3$ h there is no τ dependency and a mean spread value of 0.15 indicates fairly predictable situations. In contrast, for $\tau > 3$ h the precipitation spread is larger and steadily increasing, pointing towards unpredictable weather situations. A regression line fitted for $\tau > 3$ h indicates a small positive correlation between $S_{n,P}$ and τ ($R^2 = 0.12$) and confirms the visual impression of a trend in weakly
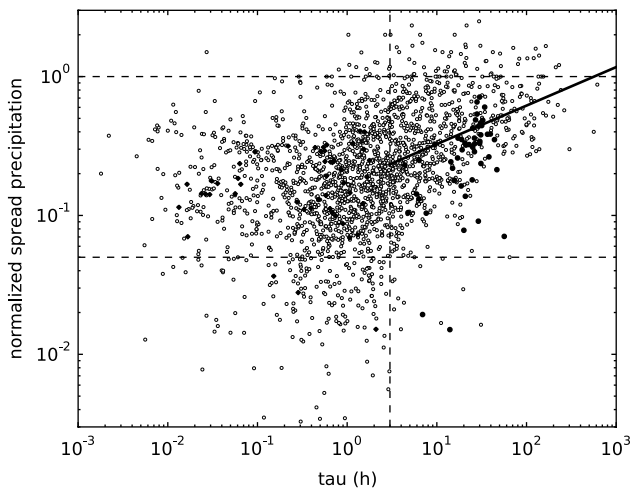
Figure 2. Scatterplot of the normalized spread of hourly precipitation at all lead times plotted against the respective convective adjustment time-scale τ for summer 2009. For the weak forcing regime ($\tau > 3$ h) a regression line is fitted to the data. The dashed horizontal lines mark characteristic values of $S_{n,P} = 0.05$ denoting good and $S_{n,P} = 1$ poor predictability, respectively (Hohenegger *et al.*, 2006), whereas the dashed vertical line marks the chosen τ threshold of 3 hours. The filled symbols represent data points of the case-study presented in section 5 denoting filled circles for the weakly and filled diamonds for the strongly forced conditions.

forced conditions (Figure 2). Note that the very short time-scales indicate non-convective precipitation merging into stratiform precipitation with embedded convection.

To assess weather regime dependent differences in forecast quality the ensemble mean of two deterministic scores is presented as a function of τ (Figure 3). For this purpose, the FBI and ETS values of individual members are computed using a radar reflectivity threshold of 19 dBZ (corresponding to 1 mm h^{-1}) before averaging. The mean FBI appears to be decreasing with increasing τ (Figure 3(a)). Although there is considerable scatter in precipitation forecast quality, a closer inspection reveals important regime-dependent differences. Applying, again, a threshold of 3 hours for τ it is evident that during strong synoptic forcing ($\tau < 3$ h) the model is predominantly overestimating the relative frequency of precipitation (FBI > 1). Conversely, it is mostly underestimated during weakly forced weather regimes (FBI < 1). Likewise, the ensemble mean ETS is generally larger (but still very low) during strong forcing conditions indicating a superior forecast quality (Figure 3(b)). The skill drops off rapidly for $\tau > 3$ h. This points towards the known problems with insufficient triggering mechanisms in COSMO-DE during weak synoptic forcing (Baldauf *et al.*, 2011; Craig *et al.*, 2012) resulting in an underestimation of precipitation and difficulties in predicting the exact location of individual convective cells.

Thus, when precipitation is controlled by synoptic forcing it is more predictable with a higher forecast quality than during weak synoptic forcing.

4.3. Impact of different sources of uncertainty on predictability

The multi-parameter and multi-boundary approach followed in COSMO-DE-EPS facilitates a disentanglement of the different sources of uncertainty by examination of various sub-ensembles depending on their perturbation type. To investigate the regime dependence, the normalized spread
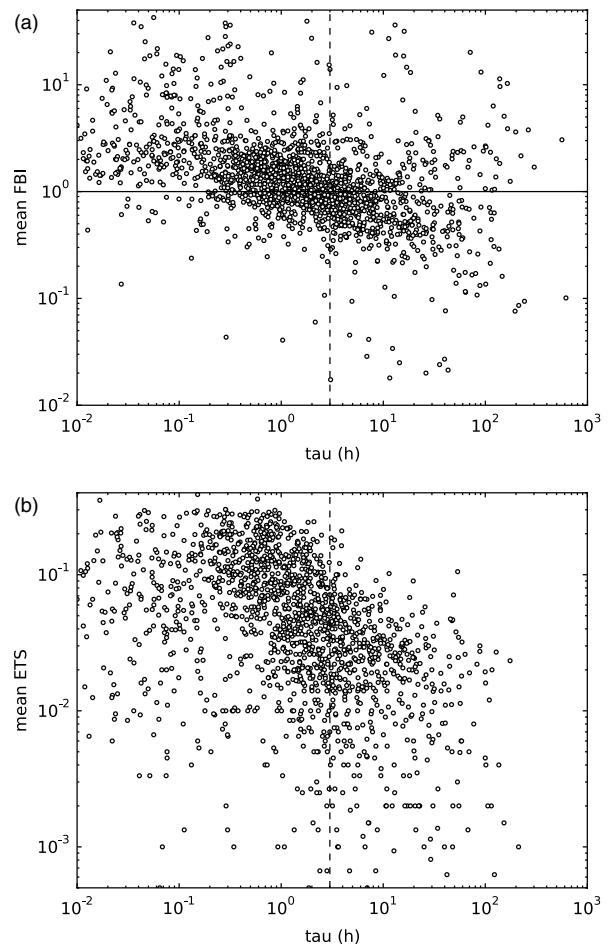
Figure 3. Scatterplot depicting the ensemble mean (a) FBI and (b) ETS of hourly instantaneous radar reflectivity as a function of convective adjustment time-scale τ. The dashed vertical line marks the τ threshold of 3 hours to stratify strong and weak forcing conditions.

of sub-ensembles is depicted depending on binned convective adjustment time-scale using box and whisker diagrams (Figure 4). The normalized precipitation spread $S_{n,P}$ of the PHY sub-ensembles is compared with the spread of the LBC sub-ensembles. The median and the quartiles of $S_{n,P}$ of the PHY sub-ensembles show a clear dependence of τ, that is, the uncertainty introduced by the physics perturbations is weather regime dependent. In the case of strong synoptic-scale forcing (small τ) the practical predictability is high (low $S_{n,P}$) and decreasing (larger $S_{n,P}$) with increasing τ. In contrast, the uncertainty introduced by the boundary conditions represented by the LBC sub-ensembles shows almost no regime dependence. The median of the LBC sub-ensembles spread of hourly precipitation rates remains fairly constant ($S_{n,P} = 0.5$ for $\tau < 10$ h) with a weak increase for larger τ (up to $S_{n,P} = 0.9$), whereas the median of the PHY sub-ensembles increases by more than one order of magnitude (from $S_{n,P} = 0.02$ to $S_{n,P} = 0.4$) indicating a strong regime dependence.

5. Weak and strong forcing case-studies

Finally two representative days of each flow regime are examined in detail to highlight the different evolution of the convective adjustment time-scale next to its ingredient CAPE and hourly precipitation rate during the course of a day. This is complemented with time series depicting the
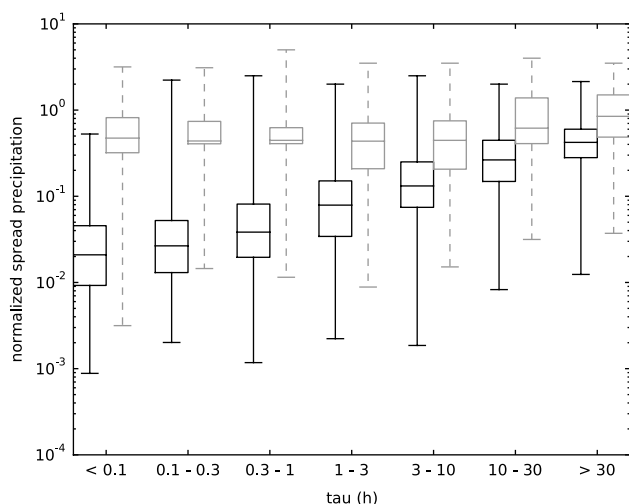
Figure 4. Normalized spread of hourly precipitation of the mean of the two sub-ensembles PHY (black) and LBC (grey) as a function of convective adjustment time-scale τ for summer 2009. The box and whisker diagrams exhibit the median, the 25 and 75 percentiles and the minimum and maximum within every bin. The bin width has been chosen to be equidistant in logarithmic scale. Note that PHY and LBC sub-ensembles are slightly offset to increase readability.

forecast quality based on instantaneous radar reflectivity of the individual ensemble members, which clearly show the clustering of the different members depending on the source of uncertainty and the differences in spread seen in the previous section.

5.1. Weak forcing

On 30 June and 1 July, weather across central Europe was influenced by an upper-level ridge and a surface high-pressure region across the North Sea leading to a weakly northerly flow and weak gradients of equivalent potential temperatures at 850 hPa (not shown). The daily accumulated precipitation field is characterized by a spotty, popcorn-like precipitation structure with large gradients and maxima close to 100 mm, typically for such locally forced precipitation episodes.

The diurnal cycle of forecast ensemble mean area-averaged precipitation, CAPE and τ highlights their typical development (Figure 5). Strongest precipitation is forecast between 1200 and 2100 UTC with a maximum around 1600 UTC (peaking in 0.2 mm h^{-1}) when the absolute precipitation spread is largest, too. CAPE exhibits a sharp increase following the solar insolation until it peaks around midday (500 to 700 J kg^{-1}), followed by a slight decrease due to latent heat release by precipitation until sunset and a larger decrease thereafter. The evolution of τ is dominated by the strong increase in the late morning when CAPE is produced but convection is not yet triggered. After the onset and the strengthening of convective precipitation, τ rapidly decreases until a minimum is reached when precipitation intensity peaks. Thereafter, τ gradually increases again while precipitation weakens. Generally, the ensemble mean area-averaged τ continuously exceeds 3 hours attaining maximum values of up to 60 hours.

The time series of the precipitation forecast quality is displayed in Figure 5(b) by using the same line style to show the members comprising a certain LBC sub-ensemble and the same colour to highlight the ones of a certain

PHY sub-ensemble, respectively. All ensemble members are evaluated in a deterministic sense using the FBI to assess their different quality. In general, three different periods can be distinguished. First, precipitation is strongly overforecast until 0900 UTC, when the ensemble predicts rainfall in a few isolated regions but hardly any precipitation is observed (not shown). Second, the precipitation is strongly underestimated between 1000 and 2100 UTC, when convection is most active and strongest precipitation is observed and predicted. Third, after 2100 UTC precipitation is overestimated when precipitation intensities are ceasing. Since the high precipitation rates in the convective period are decisive for the daily accumulation, this period doubtlessly comprises the most interesting hours. During the main convective period, the forecast quality of the individual members is controlled by the physics perturbations, and the individual members are grouped accordingly (Figure 5(b)). For instance, the members with the lowest forecast skill (FBI < 0.25, i.e. strong underestimation) during the convective period stem from the perturbation of the mixing length in the turbulence scheme (sub-ensemble LBC5). Instead of the currently operationally used value of 150 m, an asymptotic mixing length of 500 m (as was used in COSMO-DE in 2007 (e.g. Keil and Craig, 2011)) is used for members 5, 10, 15 and 20 resulting in a strong underestimation. This is in agreement with Baldauf *et al.* (2011) who showed that a smaller mixing length value, affecting the dissipation, the vertical transport, the vertical gradients and, eventually, the stability of the atmosphere, leads to superior forecast quality. The application of the ETS measure results in very poor scores (ETS < 0.05), but confirms that the physics perturbations are controlling the forecast quality (not shown). Most importantly, the main convective period (1200 until 1800 UTC) corresponds to the time window when peak precipitation occurs and the different physics parametrizations are most active resulting in the clear grouping in LBC sub-ensembles tantamount to a large spread in the PHY sub-ensembles even at forecast lead times of 12 to 18 hours.

5.2. Strong forcing

Two days in mid-July are chosen to examine forced frontal precipitation cases controlled by strong synoptic forcing. On both days the meteorological situation is characterized by an upper-level trough in conjunction with a surface low-pressure system over the British Isles with its frontal system crossing central Europe in the course of the day. The prevailing mid-level wind is westerly, and strong gradients in equivalent potential temperature at 850 hPa exist in the frontal zone (not shown). Although instantaneous radar imagery shows a convective precipitation signature, the structure of the 24 h accumulated precipitation field is fairly smooth and widely spread with radar estimated precipitation sums up to 5–30 (20–60) mm on 12 (17) July, respectively.

The time series of forecast ensemble mean area-averaged precipitation (Figure 6) exhibits continuous precipitation throughout the day peaking in 0.2 mm h^{-1} between 0600 and 0900 UTC on 12 July, when both CAPE and τ are very small (5 J kg^{-1} < CAPE < 20 J kg^{-1}, τ < 1 h). On 17 July the precipitation rates are higher with two peaks amounting to 0.5 mm h^{-1} at 0600 UTC and 0.75 mm h^{-1} at 1800 UTC. Maximum CAPE values are less than 350 J kg^{-1} shortly after 1200 UTC, while the time series of τ is showing a bimodal
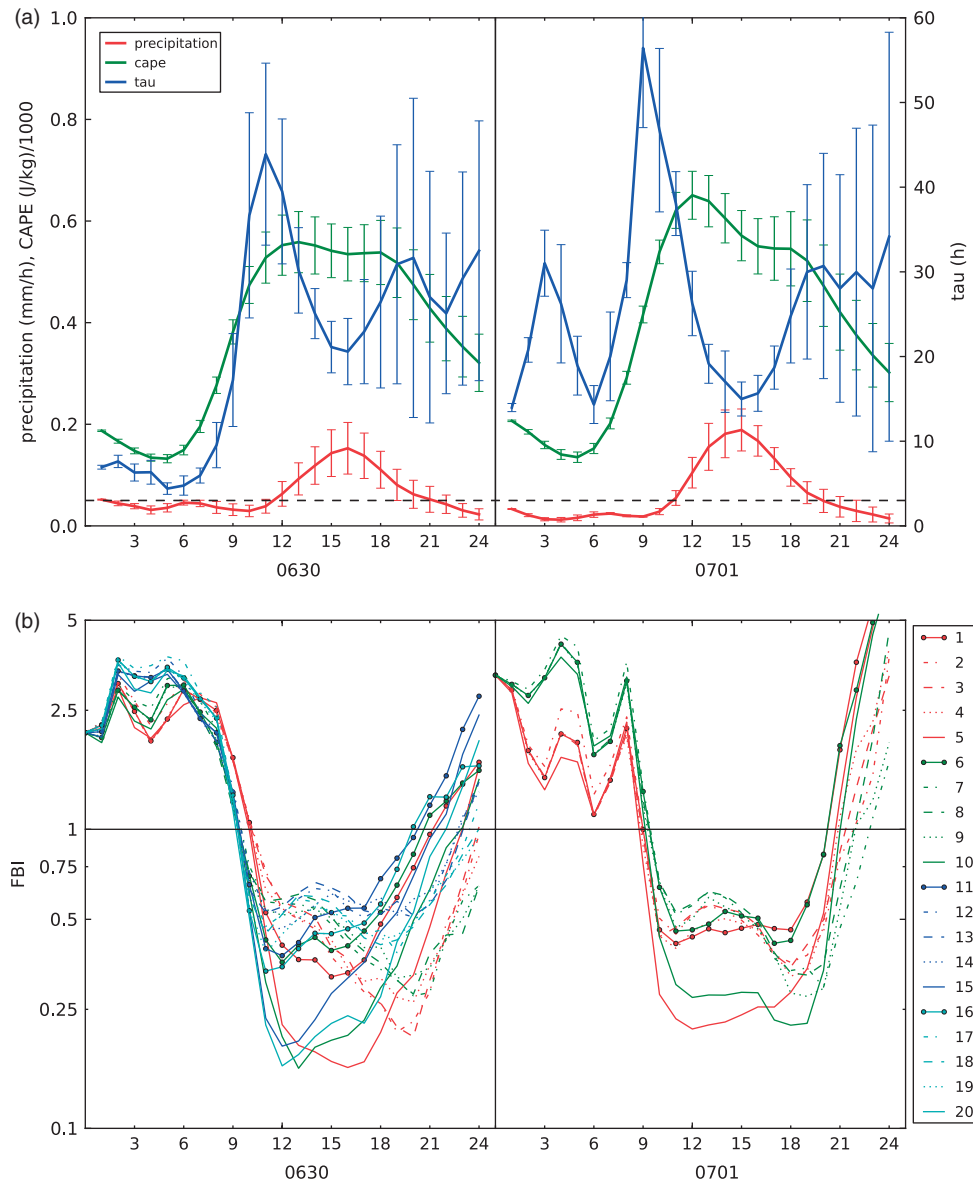
Figure 5. Time series of (a) the ensemble mean precipitation (red), CAPE (green) and the convective adjustment time-scale τ (blue) with their standard deviation and (b) the FBI of the individual members for 30 June (0630) and 1 July (0701) 2009 during weak synoptic forcing. Differently colour-coded are the PHY sub-ensembles whereas the LBC sub-ensembles are denoted with the same line style.

structure inversely to the precipitation rates. The ensemble mean area-averaged τ is less than 3 hours throughout the day. For precipitation and τ there is no diurnal cycle discernible and their temporal evolution is governed by the timing of the synoptic forcing.

The time series of FBI (Figure 6(b)) and ETS (not shown) demonstrate the dependence of the individual members on the synoptic forcing with the LBC controlling the forecast quality. The spread of the sub-ensemble containing the same physics perturbation but different LBC (e.g. sub-ensemble LBC1 consisting of members 1, 6 and 11) is large, while the spread driven with the same LBC but different physics perturbation (e.g. sub-ensemble PHY1 consisting of members 1 to 5) is negligible throughout the day. This behaviour is typical for the small τ regimes, as has been discussed for Figure 4. In comparison to the weakly forced case (compare with Figure 5(b)) the forecast quality is higher during strongly forced conditions thus confirming the results presented earlier (Figure 2). Note that on both days only 15 members are available. In summary, there is

precipitation throughout the day, τ is less than 3 h and the forecast quality is controlled by the LBC during strong synoptic forcing conditions.

6. Summary and further work

Determining different regime-dependent levels of practical predictability requires a long dataset of ensemble forecasts. Such a dataset is provided by the convection-permitting COSMO-DE-EPS covering summer 2009, when weather was characterized by frequent precipitation episodes of predominantly convective nature in central Europe.

Quantifying regime-dependent levels of predictability and forecast quality requires a measure to objectively distinguish different types of forcing of convective precipitation. The time-scale of convective adjustment τ provides a physically based measure to distinguish precipitation situations upon the degree of synoptic forcing. Based on the normalized ensemble spread of hourly total precipitation rates it is shown that the precipitation is more predictable during strong
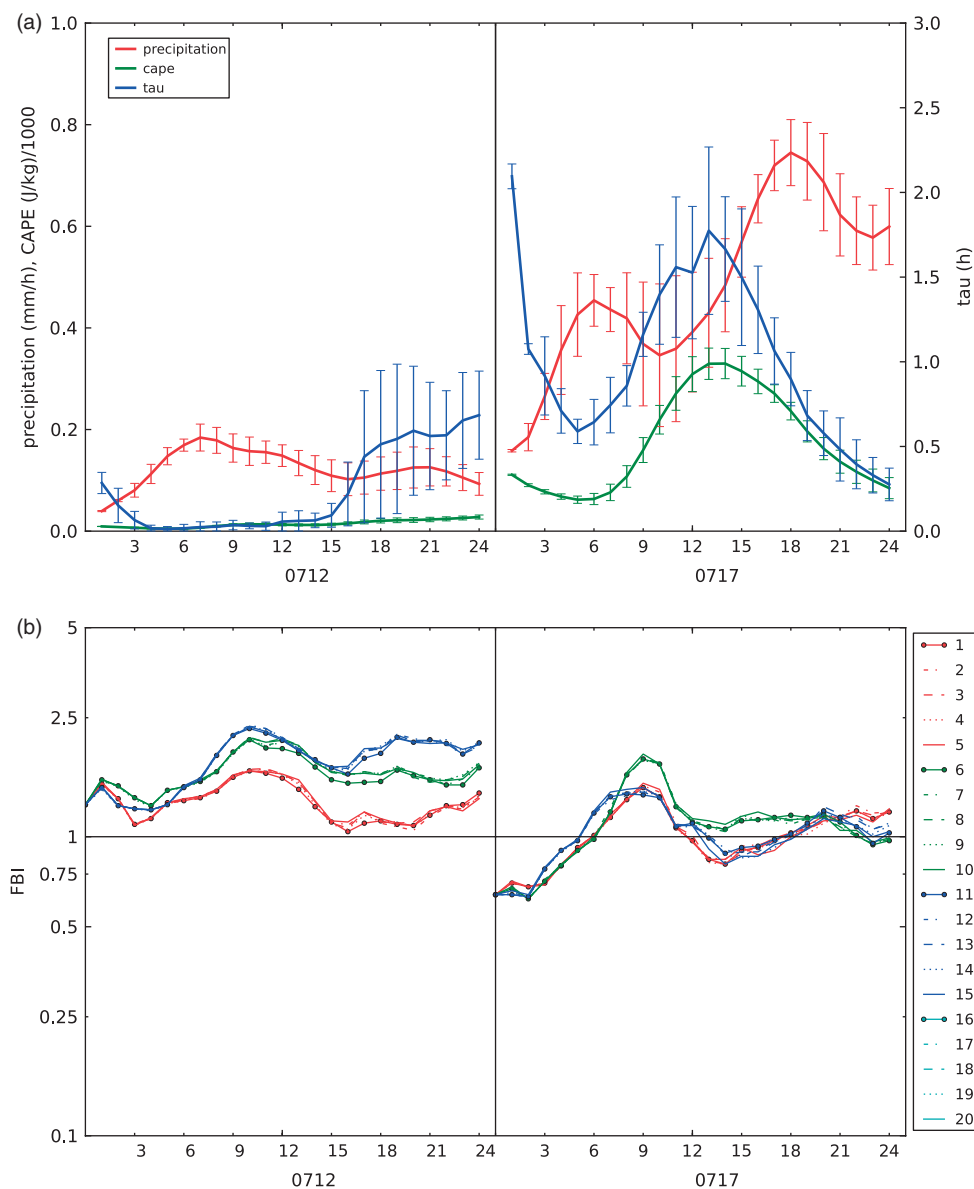
Figure 6. Same as Figure 5 but for strong synoptic forcing situations on 12 and 17 July 2009. Note that the maximum range of τ is 3 hours in (a), in contrast to Figure 5(a), where this value is illustrated by the dashed horizontal line.

synoptic-scale forcing ($\tau < 3$ h) than during weak forcing. Likewise, the forecast skill is higher during strong than during weak forcing conditions. However, the application of the convective adjustment time-scale on hourly model forecast data gives no clear separation between both weather regimes, and a continuum in the predictability of convection as suggested by Zimmer *et al.* (2011) using observations seems to exist.

Examining distinct sources of uncertainty requires an appropriate ensemble set-up. The design of COSMO-DE-EPS following a multi-parameter and multi-boundary approach facilitates such a distinction by considering certain sub-ensembles. It is found that the impact of variations in the lateral boundary conditions is quite insensitive to the prevailing flow regime, while the impact of physics perturbations is clearly regime dependent, exhibiting a strong contribution during weakly forced conditions only. Then convective precipitation turns out to be particularly sensitive to variations in the physics parametrization, that represent the model error, during the main convective period at lead times of 12 to 18 hours, when the different

parametrizations are likely most active resulting in the most spread increase.

Using hourly precipitation rates allows for the examination of the diurnal cycle of precipitation and τ during different flow conditions and highlights the results gained with the normalized spread in detail. Note that the hourly precipitation rates and, even more so, the instantaneous radar intensities used to assess forecast quality of precipitation with a mosaic of radar observations pose stringent requirements on correct location and timing of the forecasts, in contrast to frequently used rainfall accumulations over 6, 12 or even 24 hours. The longer the accumulation period the less variable and informative are the scores, and the diurnal cycle in particular is obscured.

In general the results on the weather regime dependence of precipitation forecast quality and its inherent uncertainty confirm previous ensemble studies (e.g. Stensrud *et al.*, 2000; Schwartz *et al.*, 2010; Vié *et al.*, 2011). However, an objective measure to classify the flow regime is desirable for long periods or operational applications, whereas a subjective classification of the type of forcing is only feasible

for short periods or single case-studies (e.g. Stensrud *et al.*, 2000; Vié *et al.*, 2011). The convective adjustment time-scale τ constitutes such an objective measure that is based on predicted CAPE and precipitation rates and thus easy to compute throughout the entire forecast range. Most importantly, the convective adjustment time-scale τ represents an indicator of the practical predictability level of convective precipitation, in contrast to other instability indices (like the moist Brunt–Väisälä frequency) that exhibit poor predictive skill (Hohenegger *et al.*, 2006).

In the present study the ensemble mean τ has been spatially averaged across central Europe. The spatial averaging is considered to be a significant limitation when different weather conditions coexist over different parts of the domain. Issues such as the size of the averaging domain, the usage of radar-based, quality-controlled, hourly precipitation products to assess forecast quality, the application of spatial and probabilistic verification measures and the role of initial condition perturbations are beyond the scope of the present study but are currently examined within the Hans-Ertel-Centre for Weather Research at Ludwig-Maximilians-Universität.

Here, the weather regime dependent aspect of practical predictability using quasi-operational convection-permitting ensemble forecasts of total precipitation with a limited representation of uncertainty sources has been examined. An interesting extension will be to explore the utility of the convective adjustment time-scale in intrinsic predictability experiments. We are currently investigating the aspect of intrinsic predictability by performing upscale error growth experiments with COSMO-DE applying the 3-stage-error-growth model (Zhang *et al.*, 2007) to a real weather system.

Finally, the importance of the role of the model error during the convective period in the afternoon at long lead times in weakly forced weather regimes has implications for the design of future convective-scale ensemble systems. Recent studies (Vié *et al.*, 2011; Craig *et al.*, 2012; Peralta *et al.*, 2012; Kühnlein *et al.*, 2013) demonstrate that initial condition perturbations fade out after 6 to 12 hours lead time. A future convective-scale ensemble system relying on LBCs of a global EPS combined with initial condition perturbations generated with a Local Ensemble Transform Kalman Filter (Reich *et al.*, 2011) seems to need an additional source of uncertainty representing the model error (such as a stochastic boundary-layer parametrization) especially during weakly forced conditions.

Acknowledgements

References

Baldauf M, Seifert A, Förstner J, Majewski D, Raschendorfer M, Reinhardt T. 2011. Operational convective-scale numerical weather prediction with the COSMO model: Description and sensitivities. *Mon. Weather Rev.* **139**: 3887–3905.

Barthlott C, Burton R, Kirshbaum D, Hanley K, Richard E, Chaboureau J-P, Trentmann J, Kern B, Bauer HS, Schwitalla T, Keil C, Seity Y, Gadian A, Blyth A, Mobbs SD, Flamant C, Handwerker J. 2011. Initiation of deep convection at marginal instability in an ensemble of mesoscale models: A case-study from COPS. *Q. J. R. Meteorol. Soc.* **137**(S1): 118–136.

Bei NF, Zhang FQ. 2007. Impacts of initial condition errors on mesoscale predictability of heavy precipitation along the Mei-Yu front in China. *Q. J. R. Meteorol. Soc.* **133**: 83–99.

Bowler NE, Arribas A, Mylne KR, Robertson KB, Beare SE. 2008. The MOGREPS short-range ensemble prediction system. *Q. J. R. Meteorol. Soc.* **134**: 703–722.

Clark AJ, Gallus Jr WA, Xue M, Kong FY. 2009. A comparison of precipitation forecast skill between small convection-allowing and large convection-parameterizing ensembles. *Weather and Forecasting* **24**: 1121–1140.

Craig GC, Keil C, Leuenberger D. 2012. Constraints on the impact of radar rainfall data assimilation on forecasts of cumulus convection. *Q. J. R. Meteorol. Soc.* **138**: 340–352.

Davies T, Cullen MJP, Malcolm AJ, Mawson MH, Staniforth A, White AA, Wood N. 2005. A new dynamical core for the Met Office's global and regional modelling of the atmosphere. *Q. J. R. Meteorol. Soc.* **131**: 1759–1782.

Done JM, Craig GC, Gray SL, Clark PA, Gray MEB. 2006. Mesoscale simulations of organized convection: Importance of convective equilibrium. *Q. J. R. Meteorol. Soc.* **132**: 737–756.

Done JM, Craig GC, Gray SL, Clark PA. 2011. Case-to-case variability of predictability of deep convection in a mesoscale model. *Q. J. R. Meteorol. Soc.* **138**: 638–648.

DWD. 2010. Klimastatusbericht 2009. Available at http://www.dwd.de

Errico RM, Langland R, Baumhefner DP. 2002. The workshop in atmospheric predictability. *Bull. Am. Meteorol. Soc.* **83**: 1341–1344.

Gebhardt C, Theis SE, Paulat M, Ben Bouallègue Z. 2011. Uncertainties in COSMO-DE precipitation forecasts introduced by model perturbations and variation of lateral boundaries. *Atmos. Res.* **100**: 168–177.

Hohenegger C, Lüthi D, Schär C. 2006. Predictability mysteries in cloud-resolving models. *Mon. Weather Rev.* **134**: 2095–2107.

Hohenegger C, Walser A, Langhans W, Schär C. 2008. Cloud-resolving ensemble simulations of the August 2005 Alpine flood. *Q. J. R. Meteorol. Soc.* **134**: 889–904.

Kain JS, Weiss SJ, Bright DR, Baldwin ME, Levit JJ, Carbin GW, Schwartz CS, Weisman ML, Droegemeier KK, Weber DB, Thomas KW. 2008. Some practical considerations regarding horizontal resolution in the first generation of operational convection-allowing NWP. *Weather and Forecasting* **23**: 931–952.

Kalnay E. 2003. *Atmospheric Modeling, Data Assimilation and Predictability*. Cambridge University Press: Cambridge, UK.

Keil C, Craig GC. 2011. Regime-dependent forecast uncertainty of convective precipitation. *Meteorol. Z.* **20**: 145–151.

Kober K, Craig GC, Keil C. 2013. Aspects of short-term probabilistic blending in different weather regimes. *Q. J. R. Meteorol. Soc.*, doi:10.1002/qj.2220.

Kong FY, Xue M, Thomas K, Wang Y, Brewster KA, Gao J, Droegemeier KK, Kain JS, Weiss SJ, Bright DR, Coniglio MC, Du J. 2009. 'A real-time storm-scale ensemble forecast system: 2009 Spring Experiment.' Article 16A3, *Reprints, 23rd Conf. on Weather analysis and forecasting, Omaha, Nebraska*, Am. Meteorol. Soc.: Boston, MA.

Kühnlein C, Keil C, Craig GC, Gebhardt C. 2013. The impact of downscaled initial condition perturbations on convective-scale ensemble forecasts of precipitation. *Q. J. R. Meteorol. Soc.*, submitted.

Lean HW, Clark PA, Dixon M, Roberts NM, Fitch A, Forbes R, Halliwell C. 2008. Characteristics of high-resolution versions of the Met Office Unified Model for forecasting convection over the United Kingdom. *Mon. Weather Rev.* **136**: 3408–3424.

Leuenberger D, Stoll M, Roches A. 2010. '*Description of some convective indices, implemented in the COSMO model.*' COSMO Technical Report 17, 19 pp. http://www.cosmo-model.org/content/model/documentation/techReports/docs/techReport17.pdf

Lorenz EN. 1969. The predictability of a flow which possesses many scales of motion. *Tellus* **21**: 289–307.

Lorenz EN. 2006. Predictability: A problem partly solved. pp 40–58 in *Predictability of Weather and Climate*, Palmer TN, Hagedorn R (eds). Cambridge University Press: Cambridge, UK.

Marsigli C, Montani A, Nerozzi F, Paccagnella T. 2004. Probabilistic high-resolution forecast of heavy precipitation over Central Europe. *Nat. Hazards Earth Sys.* **4**: 315–322.

Marsigli C, Montani A, Paccagnella T. 2008. 'The COSMO-SREPS ensemble for short-range system analysis and verification on the MAP D-PHASE DOP.' pp 9–14 in *Proc. Joint MAP D-PHASE Scientific Meeting-COST 731 mid-term seminar, Bologna*.

Molini L, Parodi A, Rebora N, Craig GC. 2011. Classifying severe rainfall events over Italy by hydrometeorological and dynamical criteria. *Q. J. R. Meteorol. Soc.* **137**: 148–154.

Montani A, Cesari D, Marsigli C, Paccagnella T. 2011. Seven years of activity in the field of mesoscale ensemble forecasting by the COSMO-LEPS system: Main achievements and open challenges. *Tellus* **63A**: 605–624.

Peralta C, Ben Bouallègue Z, Theis SE, Gebhardt C, Buchhold M. 2012. Accounting for initial condition uncertainties in COSMO-DE-EPS. *J. Geophys. Res.* **117**: D07108, DOI: 10.1029/2011JD016581.

Reich H, Rhodin A, Schraff C. 2011. '*LETKF for the nonhydrostatic regional model COSMO-DE.*' COSMO Newsletter **11**: 27–31.

Roberts NM, Lean HW. 2008. Scale-selective verification of rainfall accumulations from high-resolution forecasts of convective events. *Mon. Weather Rev.* **136**: 78–97.

Roebber PJ, Swanson KL, Ghorai JK. 2008. Synoptic control of mesoscale precipitating systems in the Pacific Northwest. *Mon. Weather Rev.* **136**: 3465–3476.

Rotach MW, Ambrosetti P, Ament F, Appenzeller C, Arpagaus M, Bauer H-S, Behrendt A, Bouttier F, Buzzi A, Corazza M, Davolio S, Denhard M, Dorninger M, Fontannaz L, Frick J, Fundel F, Germann U, Gorgas T, Hegg C, Hering A, Keil C, Liniger MA, McTaggart-Cowan R, Marsigli C, Montani A, Mylne KR, Ranzi R, Richard E, Rossa A, Santos-Muñoz D, Schär C, Seity Y, Staudinger M, Stoll M, Volkert H, Walser A, Wang Y, Werhahn J, Wulfmeyer V, Zappa M. 2009. MAP D-PHASE: Real-time demonstration of weather forecast quality in the Alpine region. *Bull. Am. Meteorol. Soc.* **90**: 1321–1336.

Schwartz CS, Kain JS, Weiss SJ, Xue M, Bright DR, Kong FY, Thomas KW, Levit JJ, Coniglio MC, Wandishin MS. 2010. Toward improved convection-allowing ensembles: Model physics sensitivities and optimizing probabilistic guidance with small ensemble membership. *Weather and Forecasting* **25**: 263–280.

Seifert A, Beheng KD. 2006. A two-moment cloud microphysics parameterization for mixed-phase clouds. Part 2: Maritime vs. continental deep convective storms. *Meteorol. Atmos. Phys.* **92**: 67–82.

Seity Y, Brousseau P, Malardel S, Hello G, Bénard P, Bouttier F, Lac C, Masson V. 2011. The AROME-France convective-scale operational model. *Mon. Weather Rev.* **139**: 976–991.

Stensrud DJ, Bao J-W, Warner TT. 2000. Using initial condition and model physics perturbations in short-range ensemble simulations of mesoscale convective systems. *Mon. Weather Rev.* **128**: 2077–2107.

Thompson PD. 1957. Uncertainty of initial state as a factor in the predictability of large scale atmospheric flow patterns. *Tellus* **9**: 275–295.

Trentmann J, Keil C, Salzmann M, Barthlott C, Bauer H-S, Schwitalla T, Lawrence MG, Leuenberger D, Wulfmeyer V, Corsmeier U, Kottmeier C, Wernli H. 2009. Multi-model simulations of a convective situation in low-mountain terrain in central Europe. *Meteorol. Atmos. Phys.* **103**: 95–103.

Vié B, Nuissier O, Ducrocq V. 2011. Cloud-resolving ensemble simulations of Mediterranean heavy precipitating events: Uncertainty on initial conditions and lateral boundary conditions. *Mon. Weather Rev.* **139**: 403–423.

Weusthoff T, Ament F, Arpagaus M, Rotach MW. 2010. Assessing the benefits of convection-permitting models by neighborhood verification: Examples from MAP D-PHASE. *Mon. Weather Rev.* **138**: 3418–3433.

Wilks DS. 2006. *Statistical Methods in the Atmospheric Sciences*. Academic Press: New York, NY.

WMO. 2012. 'Forecast verification: Issues, methods and FAQ.' *WWRP/WGNE Joint Working Group on Forecast Verification Research*. http://www.cawcr.gov.au/projects/verification/

Zhang FQ, Snyder C, Rotunno R. 2003. Effects of moist convection on mesoscale predictability. *J. Atmos. Sci.* **60**: 1173–1185.

Zhang FQ, Odins AM, Nielsen-Gammon JW. 2006. Mesoscale predictability of an extreme warm-season precipitation event. *Weather and Forecasting* **21**: 149–166.

Zhang FQ, Bei NF, Rotunno R, Snyder C, Epifanio CC. 2007. Mesoscale predictability of moist baroclinic waves: Convection-permitting experiments and multistage error growth dynamics. *J. Atmos. Sci.* **64**: 3579–3594.

Zimmer M, Craig GC, Keil C, Wernli H. 2011. Classification of precipitation events with a convective response timescale and their forecasting characteristics. *Geophys. Res. Lett.* **38**: L05802, DOI: 10.1029/2010GL046199.